International Journal of Applied Earth Observation and Geoinformation 122 (2023) 103451

Contents lists available at ScienceDirect

International Journal of Applied Earth Observation and Geoinformation

journal homepage: www.elsevier.com/locate/jag

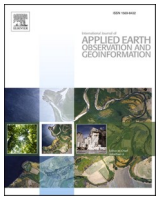

Monitoring intertidal golden tides dominated by *Ectocarpus siliculosus* using Sentinel-2 imagery

Sara Haro [a,*], Ricardo Bermejo [b,c], Robert Wilkes [d], Lorraine Bull [e], Liam Morrison [a,*]

[a] *Earth and Life Sciences, School of Natural Sciences and Ryan Institute, University of Galway, H91TK33, Ireland*
[b] *Department of Ecology and Geology, Faculty of Sciences, University of Malaga, Spain*
[c] *University of Malaga, Institute of Biotechnology and Blue Development (IBYDA), Centro Experimental Grice Hutchinson, Lomas de San Julián, 2. C.P., 29004 Malaga, Spain*
[d] *Environmental Protection Agency, John Moore Road, Castlebar F23 KT91, Co. Mayo, Ireland*
[e] *Biodiversity Officer, Parks, Biodiversity and Landscape Services, Dublin City Council, Civic Offices, Woodquay, Dublin 8 D08 RF3F, Ireland*

ARTICLE INFO

Keywords:
Remote sensing
Spectral analysis
Macroalgae
Coverage
Biomass
Environmental management
Transitional waters

ABSTRACT

Golden seaweed tides are a global environmental and social problem, that have been occurring along Ireland's eastern coastline since the 1990s. This study focused on analysing the spatiotemporal dynamics of golden seaweed (*Ectocarpus siliculosus*) coverage at Dollymount Strand in Dublin Bay (Ireland), between 2016 and 2022, and its relationship with meteorological conditions. Hyperspectral measurements in the field and Sentinel-2 imagery were utilized to monitor macroalgal blooms with a spatiotemporal resolution of 10 m and minimum costs. The normalized difference vegetation index (NDVI) values filtered between 0.1 and 1 were used to identify the coverage of golden seaweeds. The results showed that the golden seaweed coverage extended over 99% of the study area (54 ha) in June 2020 with an average NDVI of 0.25. A seasonal pattern of golden seaweed abundance was observed and modelled from May to October using a Generalized Additive Model. Approximately 28% of the coverage was correlated with daily average global radiance, and 38% of the mean NDVI was associated with daily average maximum air temperatures and wind direction by means of the Generalized Linear Models. A greater biomass of *Ectocarpus* spp. was accumulated on the beach when the wind direction was from the north-east and south-east. The results also suggested that freshwater nutrient inputs in winter from nearby estuaries may be contributing to golden tides on the shoreline. These findings are useful in developing strategies aimed at controlling and managing golden tides globally, as well as using them as bioindicators of ecological status in coastal environments.

1. Introduction

Estuarine and coastal environments are highly productive ecosystems that harbour a great variety of habitats (e.g., salt marsh plants, seagrasses, oyster beds), and provide critical regulating (primary production, nutrient cycling, blue carbon), provisioning (e.g. fish, seaweed, shellfish) and cultural (e.g. tourism, amenities) services (Cotas et al., 2023; Martin et al., 2020). Costanza et al., (1997) reported that estuaries (US$22,832 yr^{-1} ha^{-1}), seagrass meadows, and perennial seaweed forests (US$19,004 yr^{-1} ha^{-1}) are among the most valuable ecosystems in terms of services, mainly because of their crucial role in nutrient cycling (constituting more than 90% of their estimated service value). However, these ecosystems are facing various pressures due to global change, which have undermined their ecological resilience and value, leading to community shifts from highly diverse and valuable seagrass meadows or fucoid assemblages to opportunistic macroalgal blooms (Airoldi and Beck, 2007; Lotze et al., 2006). The degradation of ecological quality leading to the emergence of opportunistic macroalgal blooms and eutrophication in coastal and estuarine systems is primarily caused by several factors, including anthropogenic pollution from wastewater discharges, rising seawater temperatures due to global warming, and the introduction of non-native species through maritime transport or aquaculture (Glibert, 2017).

Eutrophication is widely acknowledged as a significant threat to aquatic ecosystems on a global scale, with far-reaching implications for the environment, society, and the economy (Liquete et al., 2013; Glibert, 2017). Over the past few decades, a significant corpus of local, regional, and international laws and conventions, such as the US Clean Water Act,

* Corresponding authors.
E-mail addresses: sara.haropaez@universityofgalway.ie (S. Haro), liam.morrison@universityofgalway.ie (L. Morrison).

https://doi.org/10.1016/j.jag.2023.103451
Received 11 May 2023; Received in revised form 14 July 2023; Accepted 6 August 2023
Available online 11 August 2023

Ramsar Convention, OSPAR Convention, and United Nations Sustainable Development Goals, have been put in place to safeguard the aquatic environment, preserve its biodiversity and other natural resources, and ensure sustainable development. In Europe, the Water Framework Directive (WFD, 2000/60/EC) and Marine Strategy Framework Directive (2008/56/EC) mark a shift in water management focus from the local to the basin scale (Apitz et al., 2006). These ambitious programs, which rely on the use of biological indicators to evaluate ecological health, place ecosystems at the forefront of management decisions (Borja, 2005). Both directives necessitate extensive monitoring and the adoption of standardized methodologies across a diverse range of environmental settings and geographic areas, placing pressure on regulatory agencies from governments to maintain monitoring costs while expanding coverage and efficacy (Carvalho et al., 2019; Hering et al., 2010).

Earth observation technologies offer enormous advantages by providing cost-effective systematic observations at large geographical scales. On the contrary, long-term monitoring through field surveys is frequently limited by its high labor and monetary costs and is characterized by lower spatial and temporal resolution. The existence of multispectral satellite imagery with higher spectral, spatial, and temporal resolutions (e.g., Landsat-8/9 or Sentinel-2) facilitates the monitoring of both water quality and seaweed tides (Bermejo et al., 2020; Schreyers et al., 2021; Sent et al., 2021; Sun et al., 2021). Currently, Sentinel-2A/B, launched in 2015, with 12 spectral bands, up to 10 m pixel resolution, and a revisit time of 2–5 days, appears to be the best available free optical sensor for monitoring and investigating intertidal vegetation from space, including seaweeds in coastal environments (Haro et al., 2022; Zoffoli et al., 2020). To achieve this objective, in-situ hyperspectral reflectance is measured to enable adequate atmospheric correction and the design of machine learning algorithms or indices that allow for the creation of intertidal vegetation maps (Borges et al., 2023; Hu et al., 2023; Roca et al., 2022).

Seaweed tides or opportunistic macroalgal blooms occur when significant quantities of rapidly growing opportunistic species accumulate (Zhang et al., 2019; Bermejo et al., 2022). These tides can have severe environmental implications, such as anoxic events resulting in mass mortality of biota and the destruction of benthic macrophytes. Additionally, seaweed tides can also pose significant socio-economic challenges, including unpleasant odours, reduced tourism, decreased amenities, and higher management costs. Seaweed tides primarily arise due to nutrient over-enrichment of aquatic ecosystems, which is usually linked with human activities (Bermejo et al., 2022; Valiela et al., 1997). Nevertheless, concurring factors such as global warming, the arrival of alien species or changes in oceanic currents are also key to understanding the occurrence and development of macroalgal blooms as these behave synergistically with eutrophication (Bermejo et al., 2023; Yoshida et al., 2015). Seaweed tides are named according to the colour of the dominant species present: green macroalgal tides (mainly *Ulva* spp.), red tides (*Gracilaria* spp.) and golden tides (e.g. *Ectocarpus* spp.; *Pilayella* spp.; *Rugulopteryx okamurae*; and *Sargassum* spp.). Traditionally, most studies have focused on green macroalgal tides dominated by *Ulva* spp. affecting estuarine environments, but more recently the number of studies reporting the occurrence of large macroalgal blooms dominated by brown seaweeds affecting coastal and estuarine areas has increased dramatically (Smetacek and Zingone, 2013). Currently, golden tides of the genus *Sargassum* spp. are affecting Chinese and Mexican coasts, the Caribbean Sea and the Gulf coast of the USA (Xing et al., 2017). In southern Europe, a large drifting biomass of the exotic macroalgae *Rugulopteryx okamurae* accumulated along the beaches of the western Alboran Sea (García-Gómez et al., 2020; Roca et al., 2022). Golden tides dominated by Ectocarpales (mainly *Ectocarpus*, *Pilayella* or *Hincksia* genus) have been reported from the Baltic (Lotze et al., 2001; Worm et al., 1999), Australia (Lovelock et al., 2008; Phillips, 2006), Massachusetts (USA; Pregnall and Miller 1988), and Ireland (Bermejo et al., 2019a; Jeffrey et al., 1993) leading to anoxic events when accumulated in large quantities.

In Dublin Bay (Ireland), species of the Ectocarpales order (mainly *Ectocarpus siliculosus*) thrive on sandy substrates, attached to the tubes constructed by the marine polychaete *Lanice conchilega* in the sublittoral zone (Jeffrey et al., 1993). These plants can grow up to 10 cm long and detach from the polychaete tubes, drifting towards the shoreline under favourable conditions such as elevated temperatures, intense sunshine, and low wind speeds. The biomass can form large accumulations of rotting seaweed on the shore, causing amenity and public health issues (Jeffrey et al., 1995, 1993; Kiirikki and Blomster, 1996). Over three decades, the presence of nuisance seaweed tides on Irish estuaries has been associated with elevated nutrient concentrations (mainly nitrogen and phosphorous). Nowadays, according to the Environmental Protection Agency only the 36 % of Irish estuaries are of high or good ecological status (EPA, 2022a, 2022b) due to eutrophication and nutrient over enrichment. In order to reach a good or high ecological status and comply with the EU WFD requirements, it is important to manage and control macroalgal blooms. The development of Earth observation technologies in combination with routine environmental monitoring (e.g. water quality, meteorological information) can provide a critical insight into understanding the development and occurrence of macroalgal blooms (Bermejo et al., 2019b; Papathanaopoulou et al., 2019; Scanlan et al., 2007).

The aim of this study was to assess the role of environmental factors (i.e. meteorological conditions and nutrient concentrations) on the occurrence of golden tides affecting the shoreline of Dollymount Strand (Dublin Bay). This general objective was divided into three specific objectives: i) to develop and validate a methodology to assess the coverage of intertidal brown seaweeds washed ashore using Sentinel-2 satellite imagery (with 10 m spatial resolution); ii) to monitor the spatiotemporal variability of golden tide abundance (coverage and average NDVI) at Dollymount Strand between 2016 and 2022; and iii) to identify the most suitable meteorological conditions promoting the occurrence of golden seaweed tides in order to anticipate actions to prevent bloom arrival or early cleaning of the beach, minimising negative impacts on the ecosystem and public use.

2. Methodology

2.1. Study area, and seaweed sampling

Dollymount Strand is a sandy beach and dune area that stretches for 5 km along the eastern shore of North Bull Island. This location has frequently been affected by golden tides, mainly consisting of *Ectocarpus siliculosus*, since the 1990s. The island is a UNESCO designated Biosphere and a Special Protection Area, surrounded by an urban landscape in Dublin Bay, located in the east of Ireland, along the Irish Sea (Fig. 1).

An initial visualization of the study area was performed on the 30th June 2022, when Dollymount beach and the River Tolka Estuary (Special Protection Area) were covered by a golden macroalgal bloom (Fig. 2). This bloom was mainly comprised of *Ectocarpus siliculosus*, although small fragments of green (*Ulva* spp.) and red seaweeds (*Polysiphonia*-like species) were also present. Subsequently, on the 6th of July, the biomass of *Ectocarpus* was measured at low tide along a transect (6 sampling points) at Dollymount Strand (Fig. 3) at the same time that the Sentinel-2 satellite flew over Dublin Bay. At each sampling point, three 30x30 cm quadrats were used to calculate the *Ectocarpus* spp. biomass. Unfortunately, excessive cloud coverage meant that the field data precluded validation using the Sentinel-2 satellite image. For this reason, *in-situ* validation was repeated on the 17th of October. Although the abundance of ectocarpoid seaweeds was considerably lower and a lower number of quadrats were collected (n = 9), the image was cloud free and the validation was performed considering three ectocarpoid seaweed patches present on the beach (see supplementary material A1).

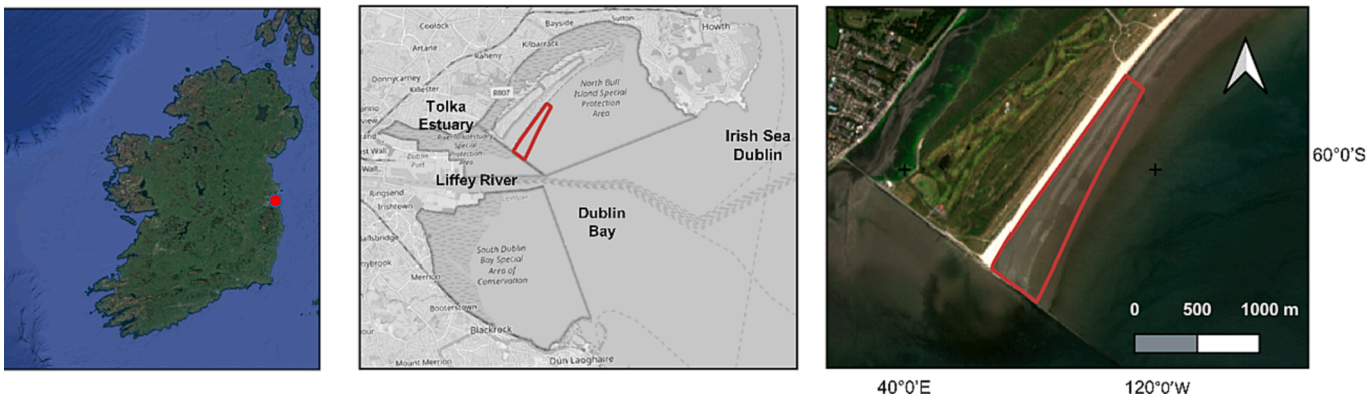

Fig. 1. Study area: intertidal area in Dollymount Strand (delimited by a red line, covers 59.4 ha), which is located in Dublin Bay (Irish Sea). The River Liffey, River Tolka, and various smaller rivers and streams flow into in Dublin Bay (Ireland). (For interpretation of the references to colour in this figure legend, the reader is referred to the web version of this article.)

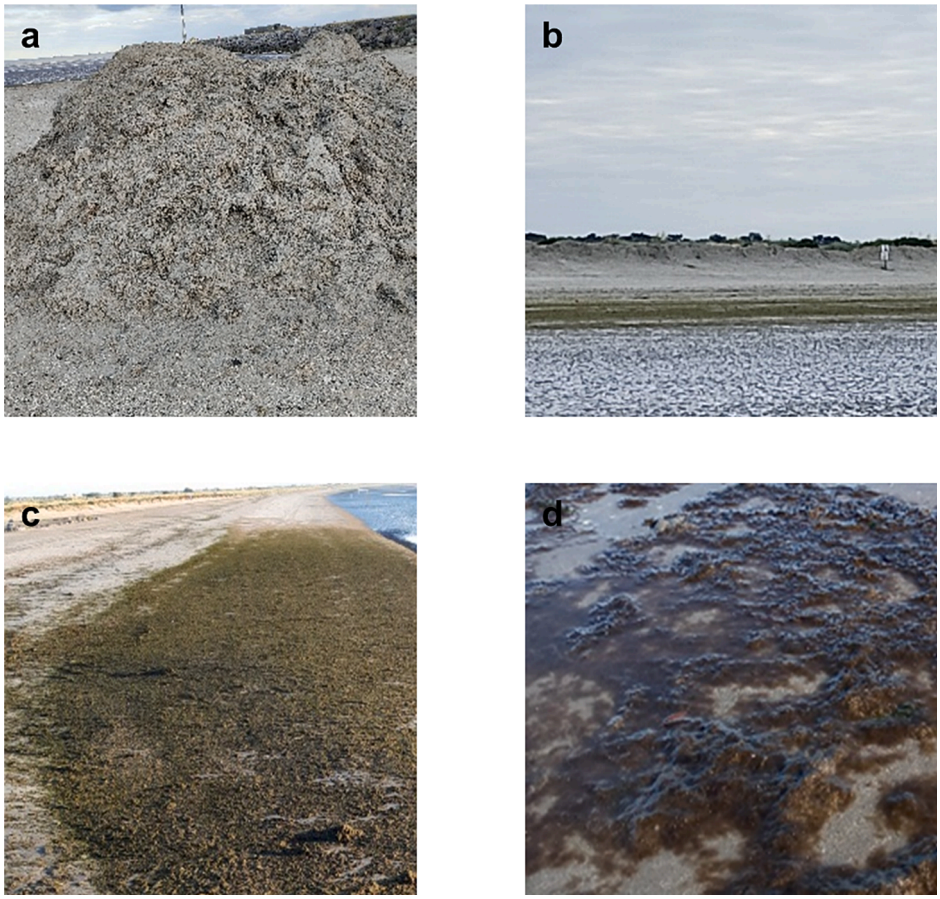

Fig. 2. Golden seaweed tides, i.e. *Ectocarpus* spp., in Dollymount Strand in Dublin Bay on the 6th of July 2022, (a) *Ectocarpus* spp. is mechanically removed with the dead macroalgae biomass piled up on the beach at Dollymount Strand; (b, c) dry golden macroalgal mat in the upper intertidal; and (d) wet ectocarpoid biomass, saturated by water, along the intertidal zone at low tides.

2.2. Reflectance spectral analysis of ectocarpoid seaweeds

The hyperspectral reflectance of golden seaweed blooms and bare sandy sediments (without macroalgal coverage) was measured *in-situ* over the visible to near infrared wavelength range using a field spectroradiometer (GER 1500, SpectraVista Corporation) at low tide on the 6th of July 2022. The in-situ hyperspectral reflectance was measured from bare sandy sediments (without macroalgal coverage), wet biomass (saturated by water along the intertidal gradient) and dry biomass (drier in upper intertidal zone) (Fig. 2; Fig. 4). Subsequently, the NDVI were calculated from reflectance spectra as (842–665)/(842 + 665) nm. It was because NDVI is usually used as a proxy of benthic photosynthetic biomass at low tide in intertidal systems (Haro et al., 2022; Zoffoli et al., 2020). At low tide, the spectral analysis revealed that areas of bare sandy sediment yielded a NDVI values of 0.08 ± 0.01 (n = 3), while the NDVI values for the wet biomass of *Ectocarpus* (650 and 2500 g m^{-2}) were approximately 0.48 ± 0.12 (n = 3), and for drier biomass (~3600 g m^{-2}) a 0.82 NDVI value was recorded (Fig. 4). Considering this data,

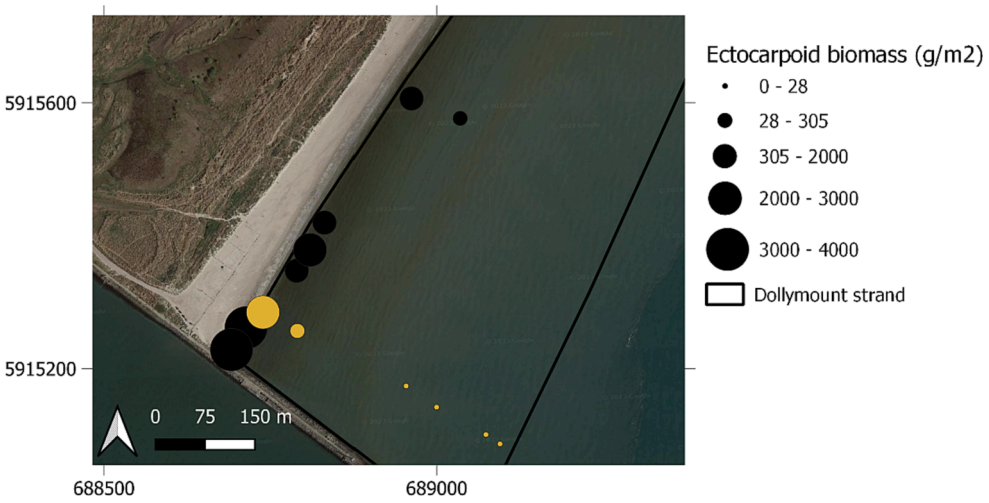

Fig. 3. Transect (yellow points) and field visualizations (black points) at Dollymount Strand the 6th of July 2022. Ectocarpoid biomass (point size), expressed as g m^{-2}, were measured at low tide. The satellite image displayed is not from July 6th. (For interpretation of the references to colour in this figure legend, the reader is referred to the web version of this article.)

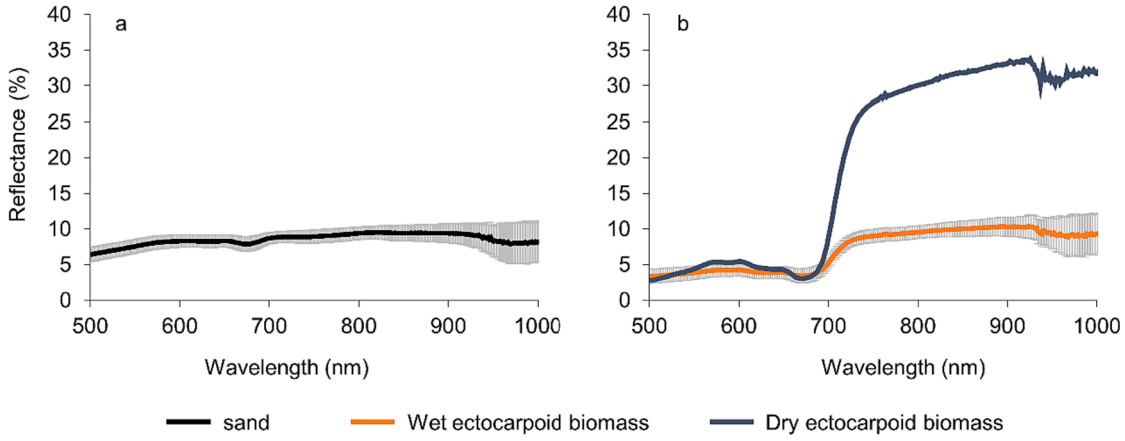

Fig. 4. *In-situ* hyperspectral reflectance measured from (a) bare sandy sediments (without macroalgal coverage), (b) wet biomass (saturated by water along intertidal gradient), and (c) dry biomass (drier in upper intertidal zone).

NDVI values higher than 0.1 were established as indicative of the presence of golden seaweeds, and these were used to map the golden seaweed bloom. This was possible due to the absence of other macrophytes, e.g. seagrasses or seaweeds, in the study area.

2.3. Satellite image processing

Sentinel-2 multispectral satellite images, cloud-free, and obtained at low tide, were manually selected from Glovis viewer. A total of 76 Sentinel-2 images (Level 2A) were analysed from 2016 to 2022. All Sentinel-2A images (Level 1C) for 2016 were download from the Copernicus Open Access Hub, and corrected for atmospheric effects using the Sen2Cor tool by Sentinel Application Platform (SNAP) toolbox. The NDVI was calculated from red and infrared reflectance bands, and values between −1 and 0.1 were removed. Google Earth Engine scripts were used to download the NDVI raster filtered between 0.1 and 1 from 2017 to 2022. For all images, the coverage of *Ectocarpus* was calculated from pixel numbers with NDVI values higher than 0.1. The average NDVI and coverage were calculated for Dollymount Strand using a shapefile (see area delimitated in red in Fig. 1). The average NDVI and the pixel numbers were calculated using the QGIS "Zonal statistics" plugin. The temporal variation of the coverage and the average NDVI of the golden tide were monitored at Dollymount Strand from 2016 to 2022. Scenes were registered in the WGS 84/UTMzone29N coordinate system (EPSG: 32629).

2.4. Meteorological data, and water quality datasets

Meteorological data was obtained from the meteorological station at Dublin Airport, located less than 10 km from the study area (Met Éireann; https://www.met.ie/; Supplementary material B1). Chlorophyll-a (Chl-a) and nutrient concentrations (i.e. dissolved inorganic nitrogen (DIN) and phosphate (PO_4^{3-})) were obtained from the monitoring programmes developed from 2019 to 2021 by the Irish Environmental Protection Agency at 26 sampling stations located nearby in the Tolka Estuary, the Liffey Estuary, Dublin Bay and the Irish Sea (Supplementary material B2).

2.5. Statistical analysis

Generalised Additive Models (GAM) were used to explore temporal trends in golden tides in relation to season and interannual variability. The coverage or average NDVI (dependent variables) were modelled as a smooth function of the independent variables "Month" or/and "Year" (predictor variables) using a spline basis with 5 degrees of freedom and a cyclic cubic smoothing type using the packages "mgcv" and "ggeffect" in

the R programmer language. Individual predictors (month and year) were estimated using type "eff", and mixed predictors (month and year) using "re". To assess the relevance of the two components of temporal variability studied (i.e. seasonal and interannual) for explaining the golden tide occurrence, all possible models were run, and the most suitable model was identified according to Akaike Information criteria (AIC). Moreover, the performance evaluation of GAMs and their accuracy metric (i.e. adjusted R-squared, deviance explained and Root Mean Square Error) for coverage and average NDVI was conducted using the "performance" package. Subsequently, Generalized Linear Models (GLM) were used to assess the correlation between meteorological data (accumulated rainfall, and daily average of maximum air temperature, highest wind speed, wind directions, and/or global radiance) and the ectocarpoid seaweed deposits (i.e. coverage and average NDVI) on the shore using the packages "glmmTMB" and "MASS" in R programmer language. To retain the variables with the best explanatory power, a stepwise AIC selection method was utilised. Meteorological variables were averaged for the previous 7 days, except for the rainfall for which the sum of the previous 7 days was calculated. In addition, wind direction was categorized based on the direction of the wind, from the sea towards the land (on-shore), from the land towards the sea (off-shore), or parallel to the shore (cross-shore). Specifically, we noted when the wind came from the northeast (NE cross-shore) or from the southwest (SW cross-shore) (See Supplementary Figure B1.2). A Kruskal-Wallis statistical analysis was performed to elucidate the impact of wind direction on the mean NDVI associated with brown seaweeds at Dollymount Strand. For this analysis, we employed the 'rstatix' package.

3. Results

3.1. Environmental conditions

Rainfall, temperature, wind speed and global radiance exhibit a clear seasonal variability over the period studied (2016–2022) (Supplementary material B1.1). The wettest months occurred between August and February. November had the highest rainfall, with an annual average of accumulated monthly precipitations of up to 528.5 mm. The monthly averages of precipitations, temperature, global radiance and the highest wind speed ranged from 1.3 to 2.5 mm, 2.4 – 20.2 °C, 178 – 1827 J cm^{-2} and 39 – 58 km h^{-1}, respectively, between 2016 and 2022. The temperature was highest from May to October (maximum monthly temperature ranged from 14 to 20 °C), and started to decrease in November, reaching an average monthly maximum of 8 °C, and minimum of 2.5 °C in January. The average monthly radiance increased from April (1354 ± 557 J cm^{-2}), reached a maximum in May (1827 ± 657 J cm^{-2}), followed by June and July (greater than 1600 J cm^{-2}), and decreasing from August to December with a global radiance of 178 ± 86 J cm^{-2}. The wind direction was primarily from the SW and NW (Fig. 5a). The monthly average wind speed oscillated between 16 km h^{-1} in July, and 23 km h^{-1} in February with gusts of up to 119 km h^{-1} (Supplementary Fig. B1.1c).

The annual average for DIN concentrations in surface waters for 2019, 2020 and 2021 were significantly higher in winter than summer in the lower Liffey Estuary (1.94 vs 0.91 mg/L), Tolka Estuary (2.05 vs 0.96 mg/L) and Dublin Bay (0.34 vs 0.09 mg/L) (Fig. 6; Supplementary material B2). The PO_4^{3-} concentration was only significantly higher in winter than summer in Dublin Bay (0.04 vs 0.01 mg/L). On the contrary, the Chl-a concentrations were significantly higher in summer than winter in the lower Liffey Estuary (1.96 vs 0.64 mg m^{-3}), Tolka Estuary (3.78 vs 0.81 mg m^{-3}) and Dublin Bay (1.63 vs 0.7 mg m^{-3}).

3.2. Mapping of spatial and seasonal abundance

The biomass of golden seaweeds, i.e. *Ectocarpus* spp., deposited at low tide on Dollymount Strand on the 6th July 2022 varied between 0 and 4226 g m^{-2} (Fig. 3). The coverage of golden seaweeds on Dollymount Strand on the 17th October 2022 was 0.07 ha, and NDVI ranged between 0.1 and 0.2, covering a narrower range of biomass (from 27 to 192 g m^{-2} for the wet biomass along the intertidal, and higher than 1000 g m^{-2}, for dry biomass in the upper intertidal) (Supplementary Figure A1). Golden seaweed was accumulated on the left margin of the area on the 17th October 2022. Overall, a greater extension of golden seaweed was accumulated on the left margin of the upper shore (Fig. 7), although a clear spatial pattern was not observed. The average golden seaweed NDVI for the entire study area between 2016 and 2022 oscillated between 0.11 and 0.25 (Fig. 8). NDVI values up to 0.7 for the golden seaweeds were observed. The golden seaweeds covered an area up to 54.02 ha on the 1st of June 2020 with an average NDVI for the entire study area of 0.25 ± 0.15 (±SD). In 2021, the highest ectocarpoid coverage was observed in June and July (Fig. 7), shows a seasonal pattern that was also modelled using the analysed temporal series (Table 1; Fig. 9). This is supported by findings recorded by Dublin City Council (DCC) for the 2021 Bathing Water Quality Report and the citizen complaint list retained by DCC, which reported an enormous presence of brown macroalgae on the beach at Dollymount and Sandymount in the summer (oral communication).

3.3. Temporal abundance, and its interaction with environmental drivers

According to GAM models, the complete model (month + year) was

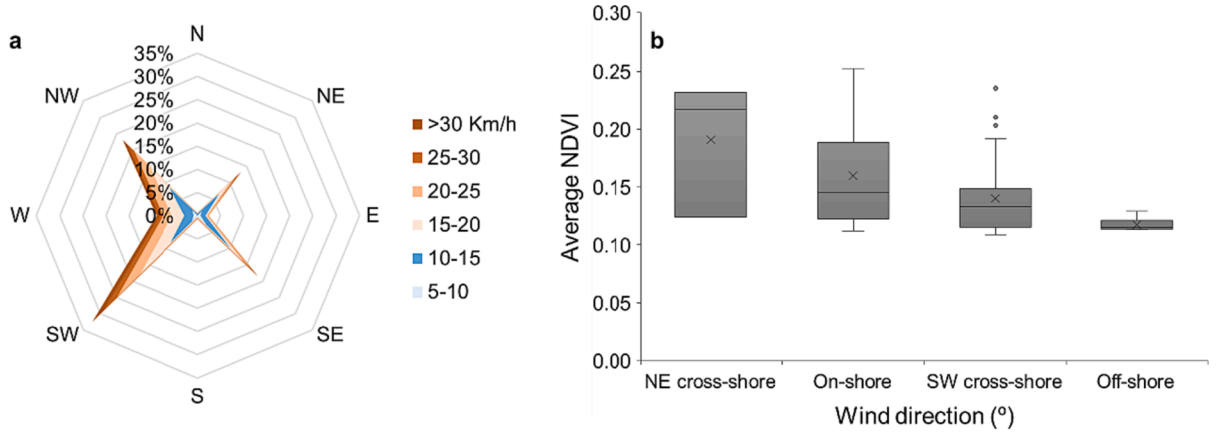

Fig. 5. a) Frequency (expressed as %) of the daily wind direction and its speed (km h^{-1}) in Dublin Bay from 2016 to 2022. Meteorological data were download from The Irish Meteorological Service (Met Éireann) a nearby meteorological station at Dublin Airport. b) The average NDVI for the study area, was categorized based on wind direction such as northeast cross-shore, on-shore, southwest cross-shore, and off-shore (see Supplementary Figure B1.2).

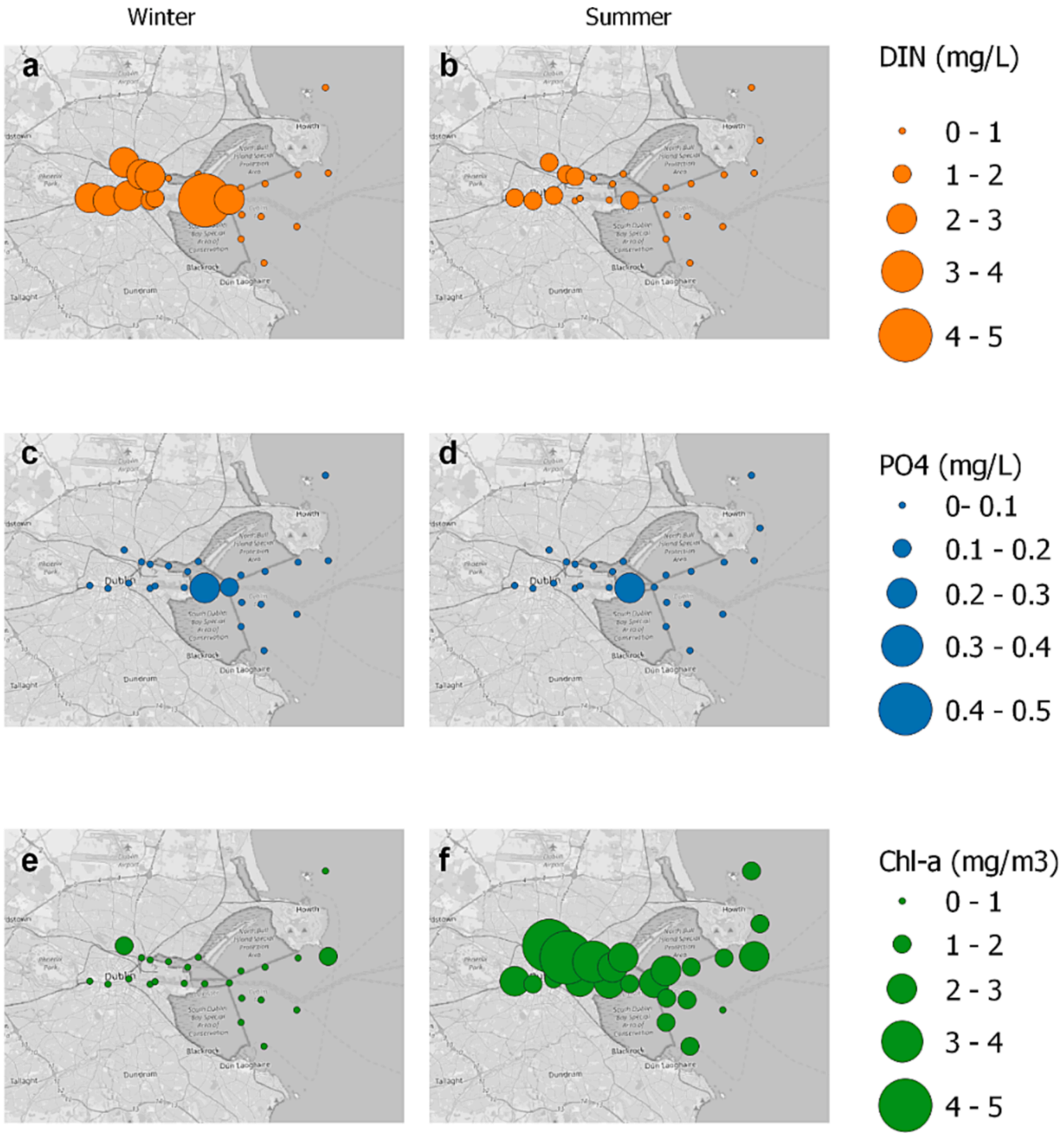

Fig. 6. Annual average concentrations of dissolved inorganic nitrogen (mg DIN L^{-1}), phosphate (mg PO_4^{3-} L^{-1}) and chlorophyll-a (mg Chl-a m^{-3}) measured at the water surface in the Tolka Estuary, Liffey Estuary, Dublin Bay and Irish Sea for winter and summer. These data were provided by the Environmental Protection Agency (EPA) (see Supplementary Figure B2). The sampling numbers oscillated between 1–4 and 1–8 for winter and summer, respectively. The standard deviation is not shown.

the most appropriate for explaining bloom coverage, suggesting a significant seasonal and interannual variability (Table 1; Fig. 9a, b). Regarding the average NDVI, the seasonal model, considering month as the only variable was the one selected based on the AIC selection criteria, indicating no interannual variability of average biomass (Fig. 9c, d). The contribution of month to golden seaweed coverage and average NDVI were significant and explained 27 % and 31 %, respectively. Interannual trends were observed in the coverage, increasing explained variability up to 37 %, when the factor year is included (predictor variables = month + year), with a AIC value of 568.1. The GAM model assessing the effect of month and year on coverage (the lowest AIC; Table 1) displayed a root mean square error (RMSE) of 9.8. This signifies that, the model's predictions deviate by approximately 9.8 units from the experimental values. With the coverage values ranging between 0 and 54 ha, the RMSE of 9.8 represents a relative error of around 18% (9.8/54) of the total coverage range.

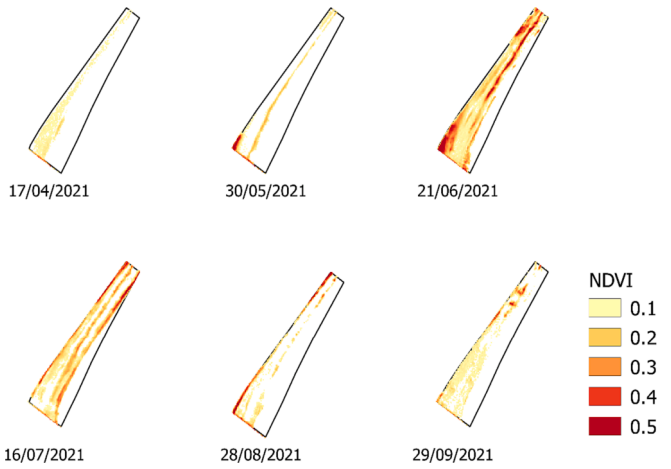

Fig. 7. Coverage and mean NDVI of *Ectocarpus* spp. in Dollymount Strand for different months in 2021 mapped from Sentinel-2 Level-2 satellite imagery using the NDVI values higher than 0.1.

The interannual effect was not observed in the average NDVI for the area studied due to the models tested (month, and month + year) being identical, with a AIC value of −290 (Table 1). Therefore, the simplest model (effect of month on average NDVI) was selected. This model achieved an RMSE of 0.035. Considering that the NDVI values ranged from 0.25 to 0.00, a RMSE of 0.035 represents a relative error of approximately 14% (0.035 / 0.25) of the total range of NDVI values.

The coverage of golden seaweeds increased in April, reached a maximum at the beginning of June (~20 ha), and decreased in October (Fig. 9a). Fig. 9b shows that the highest interannual trends in the modelled coverage occurred in 2019. The average NDVI followed a similar seasonal pattern with coverage, increasing in April and decreasing in October. However, the maximum average NDVI was modelled at the end of June (slightly lower than 0.2; Fig. 9c). A direct correlation was observed between golden seaweed coverage and average NDVI for the area examined (Pearson coefficient, r, = 0.38; n = 74; p = 0.05).

According to the AIC selection method, the GLM considering only global radiance (Rad., J cm^{-2}), was the most suitable for explaining the coverage. Approximately 28 % of the *Ectocarpus* spp. coverage variability (ha) at Dollymount Strand were explained by the daily average of global radiance (Rad., J cm^{-2}) considering the following equation: Coverage (ha) = 0.010·Rad + 1.603 (Table 2). Regarding average NDVI, the model considering maximum air temperatures (Tmax, °C) and wind direction (ddhh, deg) was the most satisfactory, and explained up to the 38 % of variability and was defined by the following equation: average NDVI = 0.107 + 0.005·Tmax – 1.71E-04·ddhm. The highest values of average NDVI for the study area were observed when the winds were onshore and from a NE cross-shore direction (Fig. 5b) (Supplementary material B2). Significant differences were revealed by the Kruskal-Wallis statistical analysis (p-value = 0.0226). This suggests that the ectocarpoid biomass deposited on the shoreline at low tide at Dollymount Strand could be higher when the wind direction is from the north-east (~12 % days) and south-east (~18 % days) (Fig. 5a). In addition, the greatest golden seaweed abundances washed ashore in summer coincided with elevated concentrations of Chl-a at water surface (Fig. 6d) and minimum DIN concentration at all sampling locations (Fig. 6a, b). The PO_4^{3-} concentration were similar in winter and summer in the Tolka and Liffey estuaries (Fig. 6c, d).

4. Discussion

In the current study, hyperspectral reflectance from golden seaweeds was analysed, i.e. *Ectocarpus*, at low tide on the shore (Dollymount Strand, Dublin Bay, Ireland) in order to investigate the spatiotemporal abundance of golden tides using Level 2A Sentinel-2A/B multispectral imagery, and their relationship to natural and/or anthropogenic drivers (meteorological parameters, and Chl-a and nutrient concentrations at the water surface).

4.1. Golden tides mapping, and applicability of the methodology

Sentinel-2A/B imagery were useful for monitoring the presence of golden tides on the beach at low tide in absence of other macrophytes, and on a sandy substrate. These conditions are common in areas affected by seaweed tides, which makes Earth Observation a powerful tool for monitoring. In this case, an NDVI range from 0.1 to 1, which was determined from hyperspectral measurements in the field, were used to map golden seaweeds at Dollymount Strand (i.e. Ectocarpales bloom). Subsequently, this methodology was tested in southern Spain, taking

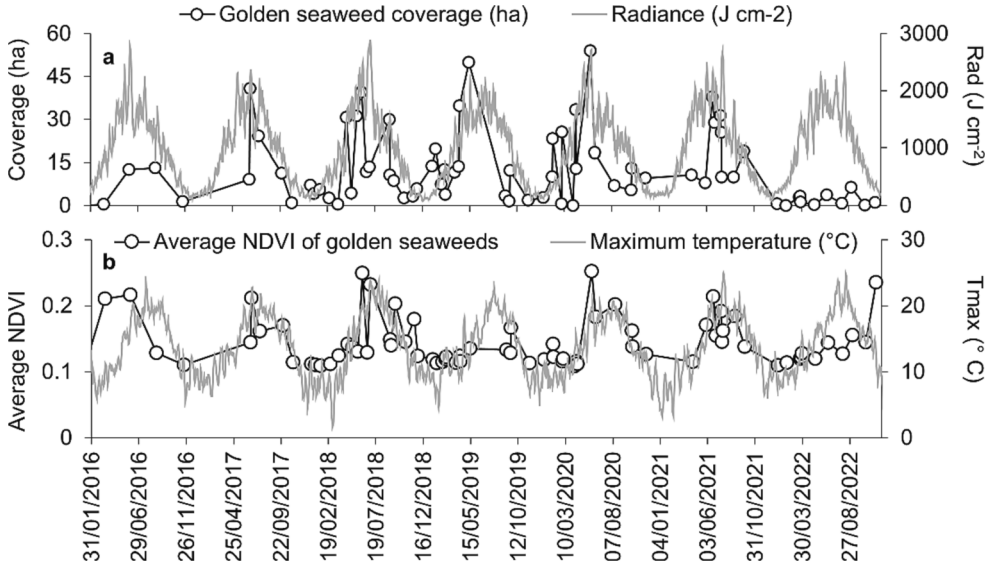

Fig. 8. a) temporal evolution of the golden seaweed coverage (ha) at dollymount strand between 2016 and 2022, and the daily average of the global radiance (rad), expressed as J cm^{-2}; b) Temporal evolution of the average golden seaweed NDVI at Dollymount Strand between 2016 and 2022, and the daily average of the maximum temperature (Tmax; °C).

Table 1
Results of the nonlinear models of golden seaweeds. Response variables: coverage and mean NDVI. Predictor variables: Month or/and Year. R^2 (adj) = adjusted R-squared; AIC = Akaike Information Criteria; Dev. Expl. = deviance explained; RMSE = root mean square error. For the Generalised Additive Models (GAM): the function s indicates non-linear smoothing splines, bs = cc is cyclic cubic smoothing, and k = 5 is the degrees of freedom.

Gam model	Parametric coefficient	Estimate	Std. Error	t value	Pr(>|t|)	R^2 (adj)	Des. Expl. (%)	AIC	RMSE
coverage ~ s(Year, k = 5, bs = "cc")						**0.091**	**12.4**	**594.0**	**11.93**
	Intercept	12.391	1.412	8.774	**5.93E-13**				
	Smooth terms	*edf*	*Ref. edf*	*F*	*p-value*				
	s(Year)	2.659	3.000	3.020	**2.29E-02**				
coverage ~ s(Month, k = 5, bs = "cc")						**0.269**	**29.1**	**577.3**	**10.73**
	Intercept	12.391	1.267	9.780	**7.75E-15**				
	Smooth terms	*edf*	*Ref. edf*	*F*	*p-value*				
	s(Month)	2.240	3.000	8.934	**6.39E-06**				
coverage ~ s(Month, k = 5, bs = "cc") + s(Year, k = 5, bs = "cc")						**0.371**	**40.9**	**568.1**	**9.80**
	Intercept	12.391	1.175	10.550	**4.47E-16**				
	Smooth terms	*edf*	*Ref. edf*	*F*	*p-value*				
	s(Month)	*2.563*	*3.000*	*11.768*	**8.90E-07**				
	s(Year)	1.879	3.000	3.668	**2.59E-03**				
NDVI ~ s(Year, k = 5, bs = "cc")						**0.000**	**1.9E-07**	**−264.3**	**0.04**
	Intercept	0.143	0.005	30.490	**<2E-16**				
	Smooth terms	*edf*	*Ref. edf*	*F*	*p-value*				
	s(Year)	0.000	3.000	0.000	**5.31E-01**				
NDVI ~ s(Month, k = 5, bs = "cc")						**0.313**	**33.6**	**−290.1**	**0.34**
	Intercept	0.143	0.004	36.770	**<2E-16**				
	Smooth terms	*edf*	*Ref. edf*	*F*	*p-value*				
	s(Month)	2.507	3.000	11.350	**1.18E-06**				
NDVI ~ s(Month, k = 5, bs = "cc")+ s (Year, k = 5, bs = "cc")						**0.313**	**33.6**	**−290.0**	**0.35**
	Intercept	0.143	0.004	36.770	**<2E-16**				
	Smooth terms	*edf*	*Ref. edf*	*F*	*p-value*				
	s(Month)	2.507	3.000	11.350	**1.18E-06**				
	s(Year)	0.000	3.000	0.000	**9.11E-01**				

advantage of the detailed study carried out by Roca et al. (2022), who mapped a golden seaweed tide dominated by *Rugulopteryx okamurae,* an invasive brown seaweed of the order Dictyotales (Strait of Gibraltar Natural Park) (see supplementary material A2). As it can be observe in the supplementary material, the results of the methodology followed in this study matched very well with those obtained by Roca et al., (2022) on Bolonia Beach the 30th June 2021 using unmanned aerial vehicles, and Sentinel-2 and Landsat-8 images, using a Support Vector Machine (SVM) supervised classification technique and NDVI. In the case of the methodology followed by Roca et al. (2022), the use of machine learning algorithms can preclude the use of her methodology in other areas, as these algorithms are complex black-box models which are often difficult to replicate in other locations (Rudin, 2019). On the contrary, the method followed on our study was easily applicable, and correctly identified the three main patches of *Rugulopteryx okamurae* washed ashore on Bolonia Beach (Tarifa, Cadiz, Spain) on that day (see Fig. 8, panel 6, Roca et al 2022). To date, the study by Roca et al 2022 is the only study in which *Rugulopteryx okamurae* was monitored using Earth Observation technologies. In addition, our study is the first in which Ectocarpales seaweeds were monitored using multispectral satellite imagery.

The majority of studies regarding golden seaweeds using remote sensing are based on monitoring *Sargassum* sp. (order Fucales) on Chinese and Caribbean coasts, and consider low spatial resolution imagery (e.g. MODIS, Sentinel-3) (Hu et al., 2015; Ody et al., 2019; Wang and Hu, 2016; Xing et al., 2017). Although, medium resolution satellite imagery (e.g. Landsat, Sentinel-2, and PlanetScope) has been used to monitor golden tides of *Sargassum* (Chávez et al., 2020; Cuevas et al., 2018; Wang and Hu, 2021), these golden tides are frequently pelagic. Thus, it is mainly monitored while floating (Cuevas et al., 2018; Chávez et al., 2020; Wang and Hu, 2021; Sun et al., 2021), and few studies have focused on Sargasso deposits on the beach (Arellano-Verdejo et al., 2022, 2019; Zhang et al., 2022). There are a multitude of vegetation indices (e.g. enhanced vegetation index (EVI), Floating Algae Index (FAI), seaweed enhancing index (SEI)), which are often computed to monitor seaweeds floating at the water surface in coastal environments using satellite imagery of low spatial resolution (e.g. AquaModis, Sentinel-3; Hu 2009, Ody et al. 2019, Siddiqui et al. 2019, Liu et al., 2021), or to monitor submerged benthic macroalgae (Vahtmäe et al., 2021), which are not fully suitable for monitoring emerged macroalgae. In our study, as the seaweed tides were monitored at low tide, the NDVI was considered for the assessment of these seaweed tides using imagery of higher spatial resolution (10 m). Similar to the work presented here, Borges et al., (2023), Roca et al., (2022), Zoffoli et al., (2020) performed NDVI estimations from hyperspectral reflectance measurements to calibrate the NDVI range from multispectral satellite imagery associated with seaweeds or seagrasses at low tides. Currently, researchers are developing methodologies based on remote sensing to assess submerged aquatic vegetation (Li et al., 2023; Vahtmäe et al., 2021). Understanding this could be essential in deciphering the causes of massive

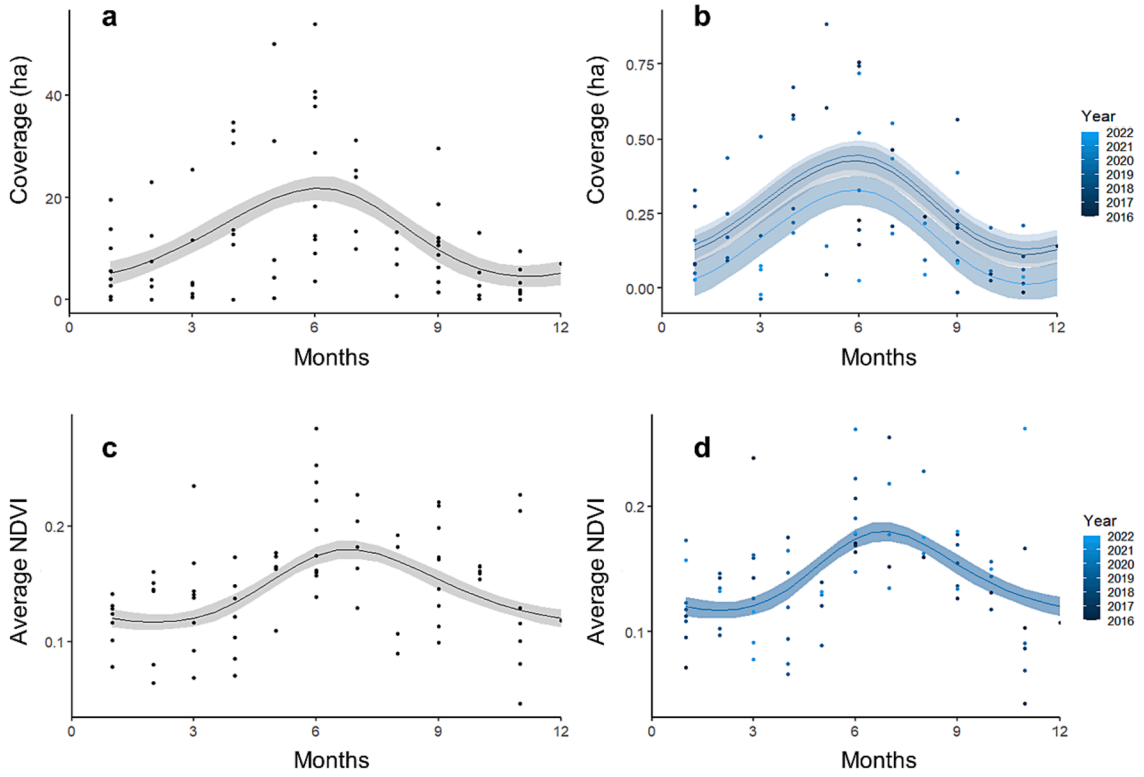

Fig. 9. (a) The non-linear effect on golden seaweed coverage of month (a), and month and year (b). The non-linear effect on average golden seaweed NDVI of month (c), and month and year (d). The coverage was normalized by maxima coverage (54.02 ha) to obtain values between 0 and 1.

Table 2
Results of the linear models of golden seaweeds. Response variables: coverage and mean NDVI. Predictor variables: accumulated rainfall (rain), daily average of maximum temperature (Tmax), daily average of the highest wind speed (wsp), daily average of global radiance (rad). For Generalized Linear Models (GLM): stepwise AIC, family = Gaussian.

glm model	Parametric coefficient	Estimate	Std. Error	t value	Pr(>|t|)	R^2	AIC
coverage ~ rain + Tmax + wsp + ddhm + rad							590.2
coverage ~ Tmax + wsp + ddhm + rad							588.3
coverage ~ Tmax + wsp + rad							586.6
coverage ~ Tmax + rad							584.9
coverage ~ rad						**0.28**	**583.9**
	Intercept	1.603	2.362	0.679	**0.499**		
	rad	0.010	0.0019	5.319	**1.07E-06*****		
NDVI ~ rain + maxtp + wsp + ddhm + rad							−285.5
NDVI ~ rain + maxtp + wsp + ddhm							−287.2
NDVI ~ rain + maxtp + ddhm							−288.9
NDVI ~ Tmax + ddhm						**0.38**	**−289.7**
	Intercept	0.107	0.023	4.560	**2.01E-05*****		
	Tmax	0.005	0.001	5.135	**2.26E-06*****		
	ddhm	−1.71E-04	0.000	−2.296	**0.0246***		

Signif. codes: 0 '***' 0.001 '**' 0.01 '*' 0.05 '.' 0.1 ' ' 1.

accumulations of opportunistic macroalgae on the shoreline, as these macroalgae typically grow submerged in the subtidal zone, being subsequently washed ashore (Jeffrey et al., 1993; Roca et al., 2022). Note that the development of methodologies to study underwater aquatic vegetation from space depends on the spectral signature of the photosynthetic community investigated and, obviously, on the optical properties of the water column, which vary depending on the specific estuary, coast, or water body (Dörnhöfer and Oppelt, 2016; Yang et al., 2022).

As in the case of the bloom forming species of Ulva, Ectocarpales seaweed mapping could be also used as to determine water quality, ecological status and the eutrophication status of European coasts and estuaries according with the WFD. The WFD standards established that opportunistic macroalgal blooms can be used as biological indicators of the ecological status of transitional waters (Papathanaopoulou et al., 2019; Wan et al., 2017). At the present, all investigations focus solely on macroalgal blooms of Ulvaceae, although Ectocarpales blooms could be also used as bioindicators of ecological status in coastal environments, such as the Irish Sea, Baltic Sea and elsewhere globally, in which eutrophication is associated with Ectocarpales blooms (Jeffrey et al., 1993; Kiirikki and Blomster, 1996; Michalak, 2020). For instance, metrics such as the percentage cover, the spatial extent of the bloom or biomass abundance are currently used to assess the ecological status of estuarine and coastal waterbodies following the methodology described by Scanlan et al., (2007). These metrics could be calculated from our maps of *Ectocarpus* spp. to develop an index to estimate the ecological status following a similar approach to that proposed by Scanlan et al., (2007) or Zoffoli et al., (2021).

4.2. Spatiotemporal dynamic, and environmental drivers

As with other primary producers, the principal environmental drivers controlling the development of opportunistic bloom forming species are light, temperature and nutrients (Lotze et al., 2001; Valiela et al., 1997). In high and middle latitudes, primary production is usually limited by light and temperature during the winter, and by nutrients during spring and summer (Bermejo et al., 2019b; McGovern et al., 2019; Wang et al., 2012). In areas where nutrient are in excess, seasonal peak blooms of golden tides occur in summer as previously reported in Denmark, South Africa and Australian, as well as on Chinese and Caribbean coasts for *Sargassum* (Gillespie and Critchley, 1999; Hoang et al., 2016; Thomsen et al., 2006), in the Azores and the Strait of Gibraltar for *R. okamuarae* (Faria et al., 2022; García-Gómez et al., 2020), along the subtropical eastern Australian coast, on the Baltic Sea Coast, in Nahant Bay in Massachusetts, and on eastern coast of Ireland for different Ectocarpales (*Ectocarpus*, *Pilayella* or *Hincksia* genus) (Jeffrey et al., 1993; Lotze et al., 2001; Phillips, 2006; Pregnall and Miller, 1988). This expected seasonal trend was also captured by the GAM model for the coverage and the average NDVI signal, however, only coverage showed a relevant interannual variation (Table 1), that may be more likely related with changes in climatic conditions or alternatively by annual differences in nutrient loadings.

The first deposits of *Ectocarpus* spp. on the beach in Dollymount Strand were described from the 17th June 1989, 21st May 1990, and 12th September 1991 (Jeffrey et al., 1993). Ectocarpoid blooms extended approximately 100 m wide and 2.5 km long with an average biomass of 4000 g m^{-2}. *Ectocarpus* spp. remained on the beaches until late July, with lesser amounts occurring until the end of September. These patterns were similar to those observed in the current study (Figs. 7-9), as well as one band with up to 4000 g m^{-2} of ectocarpoid seaweed which was observed in the upper intertidal zone on the 6th of July 2022 (Fig. 3). A small amount of this band still remained on the left margin in upper shore on the 17th of October 2022 (Supplementary Fig. A1b). However, the overall abundance of golden seaweed in summer could be higher than what observed in the current work due to frequent mechanical removal by the local council (Dublin City Council; DCC) between June and October for several years, i.e. using tractors. Unfortunately, the quantities of brown seaweeds mechanically removed in the study area is not recorded by DCC (oral communication). Jeffrey et al., (1993) associated the ectocarpoid seaweed deposits on the beach with relatively high temperatures, intense sunshine, and low wind speed. According to the current study, the ectocarpoid biomass was partially explained by the daily average of maximum air temperature (Fig. 8b), and wind direction (Fig. 5b). The increase in golden tides observed in Dublin Bay could be a consequence of positive trends in seawater warming in the Irish Sea, where the temperature has been increasing at a rate of 0.04 °C year^{-1} (Casal and Lavender, 2017). Additionally, the presence of ectocarpoid biomass washed ashore was greater when the wind blew from either the northeast or southeast, i.e., NE cross-shore and on-shore, respectively (Fig. 5b). In addition, the golden seaweed coverage seems to decrease as a consequence of low radiance (Table 2; Fig. 8a). Inverse correlations were observed between wind speed with coverage ($r = -0.27$; $n = 76$; $p = 0.05$) and average NDVI ($r = -0.39$; $n = 76$; $p = 0.05$), so conditions of strong winds could (1) deposit a layer of sand over the algal biomass leaving it buried, and/or (2) drag the golden seaweeds towards the sea when the strong winds originate from a southwesterly or northwesterly direction (Fig. 5a; Supplementary Figure B1.2). The abiotic factors (i.e., wind direction, maximum temperature, and radiance) could explain between 28 and 38 % of the abundance of *Ectocarpus* spp. deposited on the shoreline at low tide on Dollymount Strand. *Ectocarpus* spp. were likely washed on to the beach from the sublittoral zone, where *Ectocarpus* spp. grow on the tops of burrowing marine polychaetes, i.e. *Lanice*, in environments characterised by low wave energy (Jeffrey et al., 1993). Higher densities of *Lanice* could result from the availability of greater amounts of particulate organic matter, and elevated nutrient concentrations. In this study, the highest DIN concentrations in surface waters were recorded in Dublin Bay, the lower Liffey Estuary and the Tolka Estuary in winter (Fig. 6a). On the contrary, the highest golden seaweed deposits (Fig. 7) were found at minimum DIN concentration, i.e. in summer (Fig. 6b). Therefore, the lower DIN concentration at the water surface in summer in Dublin Bay and the Tolka estuary could be due to a higher consumption of nitrogen by the golden seaweed and other photosynthetic organisms, for growth. The presence of nuisance seaweeds in Dublin Bay (elevated Chl-a concentrations in water surface in summer; Fig. 6f) were previously associated with low nitrogen concentrations in the water column (Jeffrey et al., 1995; Bermejo et al., 2022). A part import of inputs loads of N and P into the estuary could came from Dublin's main sewage treatment plant, called The Ringsend Wastewater Treatment Plant (WWTP), which is overloaded and is not in compliance with the EU's Urban Wastewater Treatment Directive (EPA, 2022c). Currently, this WWTP is a significant source of DIN and PO_4^{3-}, and it is observed in the DIN and PO_4^{3-} concentrations measured in the lower Liffey Estuary all year round (Fig. 6a-d). This may be impacting on the nutrient balance and enhancing the opportunistic macroalgae proliferation.

5. Conclusions

The results presented in the current study are based on an initial case study in Ireland, which can be applied to other locations globally, affected by golden seaweeds. In this work, ectocarpoid golden tides on the beach (sandy substrate in absence other macrophytes) were monitored at low tide. This method can be easily implemented, and used to support environmental monitoring and assessment, to understand environmental problems and inform sustainable management strategies. Taking into consideration the environmental and socio-economic issues caused by ectocarpoid seaweed decomposition on the shore, ectocarpoid deposits could be used as bioindicators of ecological status in coastal environments (e.g. through the development of an index to evaluate the eutrophication status of coastal or transitional waters), and compliance with the WFD criteria. The current study is essential to estimate the percentage cover and the extent of the bloom using Sentinel-2 imagery. The use of bioindicators must be complemented with the monitoring of physico-chemical indicators. Therefore, in order to manage water quality in Dublin Bay and blooms of golden seaweeds, water quality monitoring (e.g. Chl-a, turbidity, etc.) along the Irish coastline could be enhanced by using Sentinel-2 imagery coupled with periodic *in-situ* sampling campaigns. This would permit the estimation of water quality every 5 days if meteorological conditions were suitable. This is especially relevant considering the current pressures from governments on their regulatory agencies to comply with environmental monitoring requirements associated with the implementation of European Directives such as the WFD or the MSFD. In the current study, a seasonal trend in the abundance of ectocarpoid seaweed washed ashore was only partially explained by meteorological parameters (maximum air temperature, radiance, and wind direction). Therefore, other factors (e.g. *Lanice* tubes) should be studied further. Moreover, to manage the blooms of golden tides occurring in coastal regions and to assess the deposits washed ashore, it is necessary to investigate ectocarpoid seaweed floating at the water surface in the intertidal, and attached to the substrate in the sublittoral zone. The present study establishes a novel approach for the management of brown algal tides in Europe and worldwide.

CRediT authorship contribution statement

Sara Haro: Funding acquisition, Visualization, Writing – original draft, Formal analysis, Methodology, Conceptualization. **Ricardo Bermejo:** Supervision, Visualization, Writing – review & editing, Formal analysis, Writing – original draft, Conceptualization. **Robert Wilkes:** Writing – review & editing, Resources, Conceptualization. **Lorraine**

Bull: Funding acquisition, Writing – review & editing, Resources, Conceptualization. **Liam Morrison:** Funding acquisition, Supervision, Writing – review & editing, Writing – original draft, Resources, Conceptualization.

Declaration of Competing Interest

The authors declare that they have no known competing financial interests or personal relationships that could have appeared to influence the work reported in this paper.

Data availability

Data will be made available on request.

Acknowledgments

This research was funded by Dublin City Council. Sara Haro was funded by the postdoctoral fellowship of the *Fundación Ramón Areces "XXXIII Convocatoria para Ampliación de Estudios en el Extranjero en Ciencias de la Vida y de la* Materia*"*.

Appendix A. Supplementary material

Supplementary data to this article can be found online at https://doi.org/10.1016/j.jag.2023.103451.

References

Airoldi, L., Beck, M., 2007. Loss, Status and Trends for Coastal Marine Habitats of Europe. Oceanogr. Mar. Biol. 45, 345–405. https://doi.org/10.1201/9781420050943.ch7.

Apitz, S.E., Elliott, M., Fountain, M., Galloway, T.S., 2006. European environmental management: moving to an ecosystem approach. Integr. Environ. Assess. Manage. 2, 80–85.

Arellano-Verdejo, J., Lazcano-Hernandez, H.E., Cabanillas-Terán, N., 2019. ERISNet: Deep neural network for sargassum detection along the coastline of the mexican caribbean. PeerJ 2019, 1–19. https://doi.org/10.7717/peerj.6842.

Arellano-Verdejo, J., Santos-Romero, M., Lazcano-Hernandez, H.E., 2022. Use of semantic segmentation for mapping Sargassum on beaches. PeerJ 10, e13537.

Bermejo, R., Heesch, S., Donnell, M.O., Golden, N., Mac Monagail, M., Edwards, M., Curley, E., Fenton, O., Daly, E., Morrison, L., 2019a. Nutrient Dynamics and Ecophysiology of Opportunistic Macroalgal Blooms in Irish Estuaries and Coastal Bays (Sea-MAT). EPA Research Report No. 285. Wexford (Ireland): EPA.

Bermejo, R., Heesch, S., Mac Monagail, M., O'Donnell, M., Daly, E., Wilkes, R.J., Morrison, L., 2019b. Spatial and temporal variability of biomass and composition of green tides in Ireland. Harmful Algae 81, 94–105. https://doi.org/10.1016/j.hal.2018.11.015.

Bermejo, R., MacMonagail, M., Heesch, S., Mendes, A., Edwards, M., Fenton, O., Knöller, K., Daly, E., Morrison, L., 2020. The arrival of a red invasive seaweed to a nutrient over-enriched estuary increases the spatial extent of macroalgal blooms. Mar. Environ. Res. 158 https://doi.org/10.1016/j.marenvres.2020.104944.

Bermejo, R., Golden, N., Schrofner, E., Knöller, K., Fenton, O., Serrão, E., Morrison, L., 2022. Biomass and nutrient dynamics of major green tides in Ireland: Implications for biomonitoring. Mar. Pollut. Bull. 175, 113318 https://doi.org/10.1016/j.marpolbul.2021.113318.

Bermejo, R., Galindo-Ponce, M., Golden, N., Linderhoff, C., Heesch, S., Hernández, I., Morrison, L., 2023. Two bloom-forming species of Ulva (Chlorophyta) show different responses to seawater temperature and no antagonistic interaction. J. Phycol. 59, 167–178. https://doi.org/10.1111/jpy.13302.

Borges, D., Duarte, L., Costa, I., Bio, A., Silva, J., Sousa-Pinto, I., Gonçalves, J.A., 2023. New methodology for intertidal seaweed biomass estimation using multispectral data obtained with unoccupied aerial vehicles. Remote Sens. 15, 3359. https://doi.org/10.3390/rs15133359.

Borja, Á., 2005. The European water framework directive: a challenge for nearshore, coastal and continental shelf research. Cont. Shelf Res. 25, 1768–1783. https://doi.org/10.1016/j.csr.2005.05.004.

Carvalho, L., Mackay, E.B., Cardoso, A.C., Baattrup-Pedersen, A., Birk, S., Blackstock, K. L., Borics, G., Borja, A., Feld, C.K., Ferreira, M.T., Globevnik, L., Grizzetti, B., Hendry, S., Hering, D., Kelly, M., Langaas, S., Meissner, K., Panagopoulos, Y., Penning, E., Rouillard, J., Sabater, S., Schmedtje, U., Spears, B.M., Venohr, M., van de Bund, W., Solheim, A.L., 2019. Protecting and restoring Europe's waters: an analysis of the future development needs of the Water Framework Directive. Sci. Total Environ. 658, 1228–1238. https://doi.org/10.1016/j.scitotenv.2018.12.255.

Casal, G., Lavender, S., 2017. Spatio-temporal variability of sea surface temperature in Irish waters (1982–2015) using AVHRR sensor. J. Sea Res. 129, 89–104. https://doi.org/10.1016/j.seares.2017.07.006.

Chávez, V., Uribe-Martínez, A., Cuevas, E., Rodríguez-Martínez, R.E., van Tussenbroek, B.I., Francisco, V., Estévez, M., Celis, L.B., Monroy-Velázquez, L.V., Leal-Bautista, R., Álvarez-Filip, L., García-Sánchez, M., Masia, L., Silva, R., 2020. Massive influx of pelagic sargassum spp. On the coasts of the mexican caribbean 2014–2020: Challenges and opportunities. Water (Switzerland) 12, 1–24. https://doi.org/10.3390/w12102908.

Costanza, R., D'Arge, R., De Groot, R., Farber, S., Grasso, M., Hannon, B., Limburg, K., Naeem, S., O'Neill, R.V., Paruelo, J., Raskin, R.G., Sutton, P., Van Den Belt, M., 1997. The value of the world's ecosystem services and natural capital. Nature 387, 253–260. https://doi.org/10.1038/387253a0.

Cotas, J., Gomes, L., Pacheco, D., Pereira, L., 2023. Ecosystem services provided by seaweeds. Hydrobiology 2, 75–96. https://doi.org/10.3390/hydrobiology2010006.

Cuevas, E., Uribe-Martínez, A., Liceaga-Correa, M. de los A., 2018. A satellite remote-sensing multi-index approach to discriminate pelagic Sargassum in the waters of the Yucatan Peninsula, Mexico. Int. J. Remote Sens. 39, 3608–3627. https://doi.org/10.1080/01431161.2018.1447162.

Dörnhöfer, K., Oppelt, N., 2016. Remote sensing for lake research and monitoring - Recent advances. Ecol. Indic. 64, 105–122. https://doi.org/10.1016/j.ecolind.2015.12.009.

Epa, 2022A. Water Quality in Ireland 2016–2021. European Environment Agency, Wexford (Ireland).

Epa, 2022B. Water quality monitoring report on nitrogen and phosphorus concentrations in Irish waters 2020. European Environment Agency, Wexford (Ireland).

Epa, 2022C. Urban Waste Water Treatment in 2021. European Environment Agency, Wexford (Ireland).

Faria, J., Prestes, A.C.L., Moreu, I., Martins, G.M., Neto, A.I., Cacabelos, E., 2022. Arrival and proliferation of the invasive seaweed Rugulopteryx okamurae in NE Atlantic islands. Bot. Mar. 65, 45–50. https://doi.org/10.1515/bot-2021-0060.

García-Gómez, J.C., Sempere-Valverde, J., González, A.R., Martínez-Chacón, M., Olaya-Ponzone, L., Sánchez-Moyano, E., Ostalé-Valriberas, E., Megina, C., 2020. From exotic to invasive in record time: The extreme impact of Rugulopteryx okamurae (Dictyotales, Ochrophyta) in the strait of Gibraltar. Sci. Total Environ. 704 https://doi.org/10.1016/j.scitotenv.2019.135408.

Gillespie, R.D., Critchley, A.T., 1999. Phenology of Sargassum spp. (Sargassaceae, Phaeophyta) from Reunion Rocks, KwaZulu-Natal, South Africa. In: Sixteenth International Seaweed Symposium. Springer, Netherlands, Dordrecht, pp. 201–210. https://doi.org/10.1007/978-94-011-4449-0_23.

Glibert, P.M., 2017. Eutrophication, harmful algae and biodiversity — challenging paradigms in a world of complex nutrient changes. Mar. Pollut. Bull. 124, 591–606. https://doi.org/10.1016/j.marpolbul.2017.04.027.

Haro, S., Jesus, B., Oiry, S., Papaspyrou, S., Lara, M., González, C.J., Corzo, A., 2022. Microphytobenthos spatio-temporal dynamics across an intertidal gradient using Random Forest classification and Sentinel-2 imagery. Sci. Total Environ. 804, 149983 https://doi.org/10.1016/j.scitotenv.2021.149983.

Hering, D., Borja, A., Carstensen, J., Carvalho, L., Elliott, M., Feld, C.K., Heiskanen, A.S., Johnson, R.K., Moe, J., Pont, D., Solheim, A.L., de Bund, W., van,, 2010. The European Water Framework Directive at the age of 10: a critical review of the achievements with recommendations for the future. Sci. Total Environ. 408, 4007–4019. https://doi.org/10.1016/j.scitotenv.2010.05.031.

Hoang, T., Cole, A., Fotedar, R., O'Leary, M., Lomas, M., Roy, S., 2016. Seasonal changes in water quality and Sargassum biomass in southwest Australia. Mar. Ecol. Prog. Ser. 551, 63–79. https://doi.org/10.3354/meps11735.

Hu, C., Feng, L., Hardy, R.F., Hochberg, E.J., 2015. Spectral and spatial requirements of remote measurements of pelagic Sargassum macroalgae. Remote Sens. Environ. 167, 229–246. https://doi.org/10.1016/j.rse.2015.05.022.

Hu, C., Qi, L., Hu, L., Cui, T., Xing, Q., He, M., Wang, N., Xiao, Y., Sun, D., Lu, Y., Yuan, C., Wu, M., Wang, C., Chen, Y., Xu, H., Sun, L., Guo, M., Wang, M., 2023. Mapping Ulva prolifera green tides from space: A revisit on algorithm design and data products. Int. J. Appl. Earth Obs. Geoinf. 116, 103173 https://doi.org/10.1016/j.jag.2022.103173.

Jeffrey, D.W., Madden, B., Rafferty, B., 1993. Beach fouling by Ectocarpus siliculosus in Dublin Bay. Mar. Pollut. Bull. 26, 51–53. https://doi.org/10.1016/0025-326X(93)90599-F.

Jeffrey, D.W., Brennan, M.T., Jennings, E., Madden, B., Wilson, J.G., 1995. Nutrient sources for in-shore nuisance macroalgae: the dublin bay case. Ophelia 42, 147–161. https://doi.org/10.1080/00785326.1995.10431501.

Kiirikki, M., Blomster, J., 1996. Wind induced upwelling as a possible explanation for mass occurrences of epiphytic Ectocarpus siliculosus (Phaeophyta) in the northern Baltic Proper. Mar. Biol. 127, 353–358. https://doi.org/10.1007/BF00942120.

Li, Y., Bai, J., Chen, S., Chen, B., Zhang, L., 2023. Mapping seagrasses on the basis of Sentinel-2 images under tidal change. Mar. Environ. Res. 185, 105880 https://doi.org/10.1016/j.marenvres.2023.105880.

Liu, D., Yu, S., Cao, Z., Qi, T., Duan, H., 2021. Process-oriented estimation of column-integrated algal biomass in eutrophic lakes by MODIS/Aqua. Int. J. Appl. Earth Obs. Geoinf. 99, 102321 https://doi.org/10.1016/j.jag.2021.102321.

Lotze, H.K., Worm, B., Sommer, U., 2001. Strong bottom-up and top-down control of early life stages of macroalgae. Limnol. Oceanogr. 46, 749–757. https://doi.org/10.4319/lo.2001.46.4.0749.

Lotze, H.K., Lenihan, H.S., Bourque, B.J., Bradbury, R.H., Cooke, R.G., Kay, M.C., Kidwell, S.M., Kirby, M.X., Peterson, C.H., Jackson, J.B.C., 2006. Depletion, degradation, and recovery potential of estuaries and coastal seas. Science 80, 1806–1809. https://doi.org/10.1126/science.1128035.

Lovelock, C.E., Clegg, E., Hurrey, L., Udy, J., Moore, K., 2008. Growth and physiology of nuisance alga Hincksia sordida during a bloom in South East Queensland, Australia. J. Exp. Mar. Bio. Ecol. 363, 84–88. https://doi.org/10.1016/j.jembe.2008.06.023.

Martin, C.L., Momtaz, S., Gaston, T., Moltschaniwskyj, N.A., 2020. Estuarine cultural ecosystem services valued by local people in New South Wales, Australia, and attributes important for continued supply. Ocean Coast. Manag. 190, 105160 https://doi.org/10.1016/j.ocecoaman.2020.105160.

McGovern, J.V., Nash, S., Hartnett, M., 2019. Interannual Improvement in Sea Lettuce Blooms in an Agricultural Catchment. Front. Mar. Sci. 6 https://doi.org/10.3389/fmars.2019.00064.

Michalak, I., 2020. Seaweed resources of Poland. Bot. Mar. 63, 73–84. https://doi.org/10.1515/bot-2019-0058.

Ody, A., Thibaut, T., Berline, L., Changeux, T., André, J.M., Chevalier, C., Blanfuné, A., Blanchot, J., Ruitton, S., StigerPouvreau, V., Connan, S., Grelet, J., Aurelle, D., Guéné, M., Bataille, H., Bachelier, C., Guillemain, D., Schmidt, N., Fauvelle, V., Guasco, S., Ménard, F., 2019. From in Situ to satellite observations of pelagic Sargassum distribution and aggregation in the Tropical North Atlantic Ocean. PLoS One 14, 1–29. https://doi.org/10.1371/journal.pone.0222584.

Papathanaopoulou, E., Simis, S., Zoffoli, L.M., 2019. Satellite-assisted monitoring of water quality to support the implementation of the water framework directive. EOMORES white Pap. 28 https://doi.org/10.5281/zenodo.3463051.

Phillips, J.A., 2006. Drifting blooms of the endemic filamentous brown alga Hincksia sordida at Noosa on the subtropical east Australian coast. Mar. Pollut. Bull. 52, 962–968. https://doi.org/10.1016/j.marpolbul.2006.04.015.

Pregnall, A.M., Miller, S.L., 1988. Flux of ammonium from surf-zone and nearshore sediments in Nahant Bay, Massachusetts, USA in relation to free-living Pilayella littoralis. Mar. Ecol. Prog. Ser. 50, 161–167.

Roca, M., Dunbar, M.B., Román, A., Caballero, I., Zoffoli, L.M., Gernez, P., Navarro, G., 2022. Monitoring the marine invasive alien species Rugulopteryx okamurae using unmanned aerial vehicles and satellites. Front. Mar. Sci. 9, 1–15. https://doi.org/10.3389/fmars.2022.1004012.

Rudin, C., 2019. Stop explaining black box machine learning models for high stakes decisions and use interpretable models instead. Nat. Mach. Intell. 1, 206–215. https://doi.org/10.1038/s42256-019-0048-x.

Scanlan, C.M., Foden, J., Wells, E., Best, M.A., 2007. The monitoring of opportunistic macroalgal blooms for the water framework directive. Mar. Pollut. Bull. 55, 162–171. https://doi.org/10.1016/j.marpolbul.2006.09.017.

Schreyers, L., van Emmerik, T., Biermann, L., Le Lay, Y.-F., 2021. Spotting green tides over brittany from space: three decades of monitoring with landsat imagery. Remote Sens. 13, 1408. https://doi.org/10.3390/rs13081408.

Sent, G., Biguino, B., Favareto, L., Cruz, J., Sá, C., Dogliotti, A.I., Palma, C., Brotas, V., Brito, A.C., 2021. Deriving water quality parameters using sentinel-2 imagery: a case study in the Sado Estuary. Portugal. Remote Sens. 13, 1–30. https://doi.org/10.3390/rs13051043.

Smetacek, V., Zingone, A., 2013. Green and golden seaweed tides on the rise. Nature 504, 84–88. https://doi.org/10.1038/nature12860.

Sun, D., Chen, Y., Wang, S., Zhang, H., Qiu, Z., Mao, Z., He, Y., 2021. Using Landsat 8 OLI data to differentiate Sargassum and Ulva prolifera blooms in the South Yellow Sea. Int. J. Appl. Earth Obs. Geoinf. 98, 102302 https://doi.org/10.1016/j.jag.2021.102302.

Thomsen, M.S., Wernberg, T., Stæhr, P.A., Pedersen, M.F., 2006. Spatio-temporal distribution patterns of the invasive macroalga Sargassum muticum within a Danish Sargassum-bed. Helgol. Mar. Res. 60, 50–58. https://doi.org/10.1007/s10152-005-0016-1.

Vahtmäe, E., Kotta, J., Lõugas, L., Kutser, T., 2021. Mapping spatial distribution, percent cover and biomass of benthic vegetation in optically complex coastal waters using hyperspectral CASI and multispectral Sentinel-2 sensors. Int. J. Appl. Earth Obs. Geoinf. 102, 102444 https://doi.org/10.1016/j.jag.2021.102444.

Valiela, I., McClelland, J., Hauxwell, J., Behr, P.J., Hersh, D., Foreman, K., 1997. Macroalgal blooms in shallow estuaries: controls and ecophysiological and ecosystem consequences. Limnol. Oceanogr. 42, 1105–1118. https://doi.org/10.4319/lo.1997.42.5_part_2.1105.

Wan, A.H.L., Wilkes, R.J., Heesch, S., Bermejo, R., Johnson, M.P., Morrison, L., 2017. Assessment and characterisation of Ireland's green tides (Ulva species). PLoS One 12. https://doi.org/10.1371/journal.pone.0169049.

Wang, M., Hu, C., 2016. Mapping and quantifying Sargassum distribution and coverage in the Central West Atlantic using MODIS observations. Remote Sens. Environ. 183, 350–367. https://doi.org/10.1016/j.rse.2016.04.019.

Wang, M., Hu, C., 2021. Satellite remote sensing of pelagic Sargassum macroalgae: The power of high resolution and deep learning. Remote Sens. Environ. 264, 112631 https://doi.org/10.1016/j.rse.2021.112631.

Wang, Y., Wang, Y., Zhu, L., Zhou, B., Tang, X., 2012. Comparative studies on the ecophysiological differences of two green tide macroalgae under controlled laboratory conditions. PLoS One 7, e38245. https://doi.org/10.1371/journal.pone.0038245.

Worm, B., Lotze, H.K., Boström, C., Engkvist, R., Labanauskas, V., Sommer, U., 1999. Marine diversity shift linked to interactions among grazers, nutrients and propagule banks. Mar. Ecol. Prog. Ser. 185, 309–314.

Xing, Q., Guo, R., Wu, L., An, D., Cong, M., Qin, S., Li, X., 2017. High-resolution satellite observations of a new hazard of golden tides caused by floating sargassum in winter in the yellow sea. IEEE Geosci. Remote Sens. Lett. 14, 1815–1819. https://doi.org/10.1109/LGRS.2017.2737079.

Yang, H., Kong, J., Hu, H., Du, Y., Gao, M., Chen, F., 2022. A review of remote sensing for water quality retrieval: progress and challenges. Remote Sens. 14 https://doi.org/10.3390/rs14081770.

Yoshida, G., Uchimura, M., Hiraoka, M., 2015. Persistent occurrence of floating Ulva green tide in Hiroshima Bay, Japan: seasonal succession and growth patterns of Ulva pertusa and Ulva spp. (Chlorophyta, Ulvales). Hydrobiologia 758, 223–233. https://doi.org/10.1007/s10750-015-2292-3.

Zhang, S., Hu, C., Barnes, B.B., Harrison, T.N., 2022. Monitoring sargassum inundation on beaches and nearshore waters using PlanetScope/dove observations. IEEE Geosci. Remote Sens. Lett. 19, 1–5. https://doi.org/10.1109/LGRS.2022.3148684.

Zhang, J., Shi, J., Gao, S., Huo, Y., Cui, J., Shen, H., Liu, G., He, P., 2019. Annual patterns of macroalgal blooms in the Yellow Sea during 2007–2017. PLoS One 14, e0210460. https://doi.org/10.1371/journal.pone.0210460.

Zoffoli, L.M., Gernez, P., Rosa, P., Le, A., Brando, V.E., Barillé, A., Harin, N., Peters, S., Poser, K., Spaias, L., Peralta, G., Barillé, L., 2020. Remote sensing of environment Sentinel-2 remote sensing of Zostera noltei-dominated intertidal seagrass meadows. Remote Sens. Environ. 251, 112020 https://doi.org/10.1016/j.rse.2020.112020.

Zoffoli, L.M., Gernez, P., Godet, L., Peters, S., Oiry, S., Barillé, L., 2021. Decadal increase in the ecological status of a North-Atlantic intertidal seagrass meadow observed with multi-mission satellite time-series. Ecol. Indic. 130, 108033 https://doi.org/10.1016/j.ecolind.2021.108033.